Journal of Thermal Analysis and Calorimetry, Vol. 74 (2003) 853–866

KINETICS AND HEATS OF SUBLIMATION AND EVAPORATION OF 1,3,3-TRINITROAZETIDINE (TNAZ)

M. Sućeska [1*], *M. Rajić* [1], *S. Matečić-Mušanić* [1], *S. Zeman* [2] *and Z. Jalový* [2]

[1]Brodarski Institute – Marine Research and Special Technologies, 10000 Zagreb, Croatia
[2]Department of Theory and Technology of Explosives, University of Pardubice, 532 10 Pardubice, Czech Republic

(Received January 20, 2003; in revised form August 12, 2003)

Abstract

TNAZ (1,3,3-trinitroazetidine) is a relatively new, powerful, steam castable, strained ring explosive. Owing these characteristics it is of considerable interest to the energetic material community. A relatively high vapour pressure, volume contraction and formation of shrinkage cavities in the solidification of its melt may be considered as some of its disadvantages.

The kinetics and heats of TNAZ sublimation and evaporation were studied by the non-isothermal and isothermal thermogravimetry method. The activation energy of 94–102 kJ mol^{-1} was found for TNAZ sublimation, while the activation energy of 60–81 kJ mol^{-1} was found for TNAZ evaporation. The enthalpy of TNAZ sublimation at the melting temperature was found to be 95 kJ mol^{-1}, and the enthalpy of TNAZ evaporation equals 66 kJ mol^{-1}.

Keywords: differential scanning calorimetry, evaporation, heat of sublimation, kinetics, thermogravimetric analysis, trinitroazetidine

Introduction

TNAZ (1,3,3-trinitroazetidine), a relatively new explosive material that is of considerable interest to the energetic material community, was first prepared by Archibald and co-workers in 1990 [1]. Recently, several research groups have been trying to develop improved methods for synthesis of TNAZ, to characterise it and to learn more details about its behaviour [2–18]. This four-member ring explosive is interesting for the energetic materials community for several reasons: (a) it has density and detonation characteristics nearly that of standard high explosive HMX [4, 5], it has melting transition without decomposition at about 100°C making its melt casting possible [3, 5, 6], (c) it has oxygen balance greater than that of HMX, which results in high values of the detonation heat and temperature [3, 5], and it is thermally more stable than 1,3,5-trinitro-1,3,5-triazacyclohexane (RDX), but more reactive than 1,3,5,7-tetranitro-1,3,5,7- tetrazacycloctane (HMX) [3, 5, 7].

However, TNAZ also has some characteristics that may be considered as its disadvantages. These are relatively high rates of sublimation and evaporation and volume con-

* Author for correspondence: E-mail: suceska@hrbi.hr

1388–6150/2003/ $ 20.00

Akadémiai Kiadó, Budapest
Kluwer Academic Publishers, Dordrecht

traction and formation of shrinkage cavities in the solidification of its melt. In a previous paper [3] we have found out by using differential scanning calorimetry that TNAZ melts at about 100°C and has boiling point at about 240°C. Also, we have found out that an intensive thermal decomposition of TNAZ starts above 180°C, while an intensive sublimation was observed in the range of 70–90°C, and evaporation in the range of 100–140°C. In the same paper we observed, on the basis of thermogravimetric measurements, that under isothermal conditions a 2.5 mg TNAZ sample, placed in an open aluminium sample pan, completely sublimates at the temperature of 85°C after 7 h, while at the temperature of 105°C it completely evaporates after 1 h.

A detailed characterisation of any potential energetic material, which includes determination of its physical, chemical, detonation, thermal, and other characteristics, is a starting point for its selection and exploitation in military or civilian applications. Concerning TNAZ as a relatively new energetic material, there are a number of reports on TNAZ synthesis, chemical and physical characteristics [1–3, 5, 6, 9, 15, 18]; there are also a number of reports on the TNAZ thermal characteristics and kinetics and mechanism of its thermal decomposition [3, 7, 10–13]; however there are no sufficient data in open literature on the kinetics of TNAZ sublimation and evaporation, although relatively high rates of sublimation and evaporation of TNAZ are identified as its possible disadvantages.

In this paper we have studied the kinetics and heats of these two processes from the sample mass loss data, applying the isothermal gravimetry method.

Experimental

In the study we used TNAZ synthesised starting from *tris*(methylol)-nitro methane, formaldehyde and *tert*-butylamine, according to the route [19]. The product was purified by the crystallization from 55% ethanol. TNAZ purity was higher than 99%, controlled by IR and HPLC techniques. The melting point of TNAZ, determined by DSC, was 100.59±0.21°C.

Differential scanning calorimetry (DSC) measurements were conducted using TA Instruments apparatus, model DSC 2910. Thermogravimetry (TG) and differential thermal analysis (DTA) measurements were carried out simultaneously using TA Instruments simultaneous TG-DTA apparatus, model SDT 2960. All measurements were carried out under nitrogen purging with 100 mL min^{-1}. TNAZ samples weighing up to 3 mg, loaded in an aluminium sample pan, were used.

Temperature calibration of TG, as well as temperature and enthalpy calibration of DSC, were done using indium as a reference material.

Results and discussion

Thermal properties of TNAZ

As we have shown in our previous paper [3], the shape and the position of DSC, DTA and TG curves of TNAZ depend strongly on testing conditions applied (sample mass, heating rate, method of sample loading in a sample pan – sealed or open, etc.

It is clear from the results given in Figs 1 and 2 that the shape of DSC, DTA and TG curves, at the same heating rate, is greatly influenced by the sample mass and the method of sample loading into the aluminium sample pan.

The sharp endothermic peak visible on the DSC and DTA curves at around 100°C corresponds to TNAZ melting, while the exothermic peak visible on the DSC curve at temperatures between 215 and 265°C corresponds to TNAZ thermal decomposition.

The influence of TNAZ sample mass and the way of sample loading into the sample pan on the shape of DSC, DTA and TG curves is also clearly visible from Figs 1 and 2. For example, if 2 mg of TNAZ sample placed in an open sample pan is used, then the molten sample evaporates completely before the rapid decomposition starts (Fig. 1, curve C3). This explains why in this case there is no an exothermic peak corresponding to TNAZ decomposition. The returning of the DSC curve (curve C3) to the base line at about 176°C is due to the change of the heat capacity after the TNAZ sample evaporates completely.

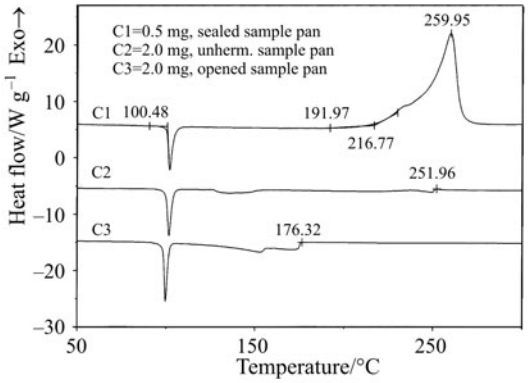

Fig. 1 DSC curves of TNAZ obtained under different testing conditions (heating rate 10°C min^{-1}, sample mass 0.5–2 mg, nitrogen atmosphere)

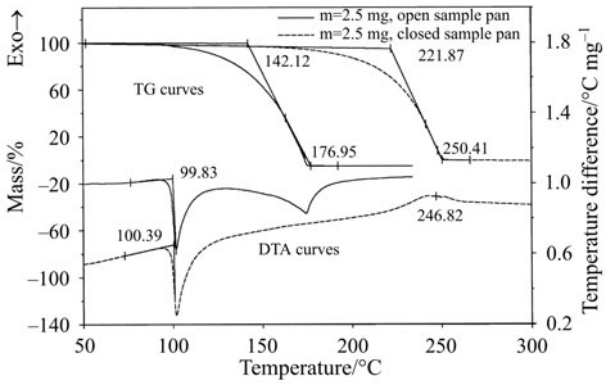

Fig. 2 TG and DTA curves of TNAZ obtained under different testing conditions (heating rate 10°C min^{-1}, sample mass 2.5 mg, nitrogen atmosphere)

The same conclusion follows from the TG and DTA curves given in Fig. 2, obtained under identical experimental conditions. The rapid loss of sample mass in the temperature range of 140–177°C is the consequence of liquid TNAZ evaporation. The sample evaporates completely up to 177°C.

The sublimation and evaporation of TNAZ may be suppressed partly using unhermetically closed (i.e. covered but not sealed) aluminium sample pans. When a TNAZ sample was tested in an unhermetically closed sample pan, it was possible to detect a small exothermic peak corresponding to the thermal decomposition, even in the case when a small sample mass was used. As it is visible from the DSC curve C2 in Fig. 1, and from the DTA curve given in Fig. 2 a small exothermic peak having a maximum at about 250°C corresponds to the exothermic decomposition of a small non-evaporated part of the TNAZ sample. An intensive sample mass loss in the range of 222–250°C, visible from the TG curve given in Fig. 2, corresponds to the exothermic decomposition. When the TNAZ samples were tested in sealed aluminium sample pans the sublimation and evaporation could be suppressed almost completely at temperatures lower than 150°C. For example, a large exothermic peak visible on the DSC curve C1 that is obtained using a closed sample pan (Fig. 1), in the range of 216–265°C, corresponds to the exothermic decomposition of TNAZ. The same is also visible from the TG curve given in Fig. 2.

Kinetics of sublimation and evaporation

It follows from Figs 1 and 2 that under non-isothermal conditions (at 10°C min^{-1} heating rate), an intensive thermal decomposition reaction of TNAZ begins above 190°C, while an intensive evaporation of molten TNAZ starts after the melting, and may under certain experimental conditions finish completely up to 180°C. From these data one may conclude that there is no overlapping of thermal decomposition and evaporation processes below 180°C. Thanks to the fact that there is no overlapping of sublimation, evaporation and decomposition, it is possible to follow each of these individual processes by the non-isothermal and isothermal thermogravimetry method, and to evaluate the kinetic parameters from the sample mass loss data.

Non-isothermal TG kinetics

The non-isothermal isoconversional model-free method developed by Flynn and Wall [20, 21] was applied to evaluate kinetic parameters of TNAZ sublimation and evaporation processes. To derive kinetic parameters, the non-isothermal TG measurements were carried out at several heating rates: 1, 2, 5, 10, 15 and 20°C min^{-1}, using 2.5 mg TNAZ samples placed in aluminium sample pans. As an example, TG and DTA curves obtained at three different heating rates are given in Fig. 3.

The kinetic parameters at different degrees of conversions (α_k) were calculated from sample mass loss data at different heating rates (β_j), from the logarithm of heating rate–temperature at which α_k conversion was reached at β_j heating rate ($T_{k,j}$) relationship, in accordance with the Flynn–Wall model-free isoconversional method [20, 21].

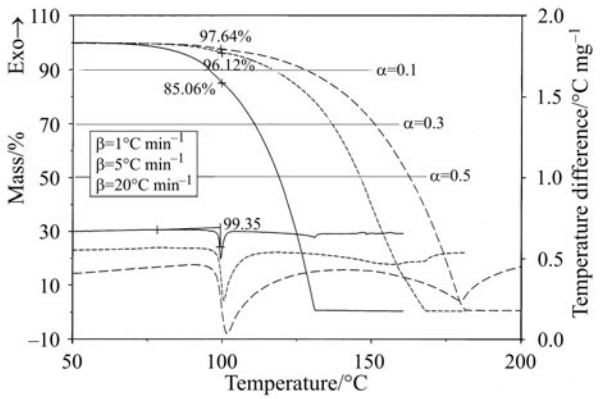

Fig. 3 Non-isothermal TG and DTA curves of TNAZ obtained at different heating rates (sample mass 2.5 mg, heating rates 1, 5 and 20°C min^{-1}, nitrogen atmosphere)

It should be noted from TG and DTA curves given in Fig. 3 that sample mass loss at the temperature region below the melting point (i.e. below 100°C) is due to TNAZ sublimation (e.g. sample mass loss at the melting point equals ~15% at 1°C min^{-1} heating rate, while at 20°C min^{-1} heating rate sample mass loss at the melting point equals ~2.4%), while mass loss at the temperature region above the melting point is due to TNAZ evaporation process. Thus, the kinetic parameters were evaluated for different degrees of conversions, taking in mind that data points for the temperature region below melting point correspond to sublimation, while data points for the temperature region above the melting point correspond to evaporation (Table 1).

Table 1 Kinetic parameters of TNAZ sublimation and evaporation at different degrees of conversion

Temperature range/°C	Conversion	Activation energy/kJ mol^{-1}	Pre-exponential factor/s^{-1}
$T_{k,j}<T_m$ (solid-state)	0.005	105	$1.82 \cdot 10^{11}$
	0.010	99	$2.05 \cdot 10^{10}$
	0.015	97	$8.55 \cdot 10^{10}$
	0.020	102	$4.92 \cdot 10^{10}$
	0.025	104	$9.81 \cdot 10^{10}$
	0.030	104	$8.35 \cdot 10^{10}$
	0.035	103	$8.75 \cdot 10^{10}$
	Mean value	102	$5.27 \cdot 10^{10}$
$T_{k,j}>T_m$ (liquid-state)	0.10	79	$3.10 \cdot 10^{7}$
	0.20	76	$1.18 \cdot 10^{7}$
	0.30	78	$1.77 \cdot 10^{7}$
	0.40	79	$3.03 \cdot 10^{7}$
	0.50	82	$6.79 \cdot 10^{7}$
	0.60	84	$1.23 \cdot 10^{8}$
	0.70	83	$1.05 \cdot 10^{8}$
	0.80	82	$9.16 \cdot 10^{7}$
	Mean value	81	$4.48 \cdot 10^{7}$

It follows from data given in Table 1 that the activation energy values for sublimation lie between 99 and 105 kJ mol^{-1} (mean value is 102 kJ mol^{-1} for conversions $0<\alpha<0.035$), while the activation energy values for evaporation lie between 76 and 84 kJ mol^{-1} (mean value is 81 kJ mol^{-1} for conversion $0.1<\alpha<0.8$). The fact that the values of the activation energy and pre-exponential factor are different for sublimation and evaporation processes indicates that these processes take place according to different mechanisms, while the facts that kinetic parameters for individual process (sublimation or evaporation) do not change significantly with conversion, indicate that mechanisms of remain unchanged with conversions.

Isothermal TG kinetics

To derive kinetic parameters of sublimation and evaporation processes from isothermal TG measurements, experiments were carried out at several temperatures in the range of 75–140°C. TNAZ samples weighing 2.5 mg, placed in opened aluminium sample pans were used in the experiments. The experiments were carried out under nitrogen flowing with 100 mL min^{-1}, in the following way. A selected isothermal temperature was programmed and when it got stabilised the apparatus furnace was opened and the sample was inserted in the sample holder. The furnace was then closed and recording of data was started at the same time.

As an example a few isothermal TG curves obtained in this way are given in Fig. 4.

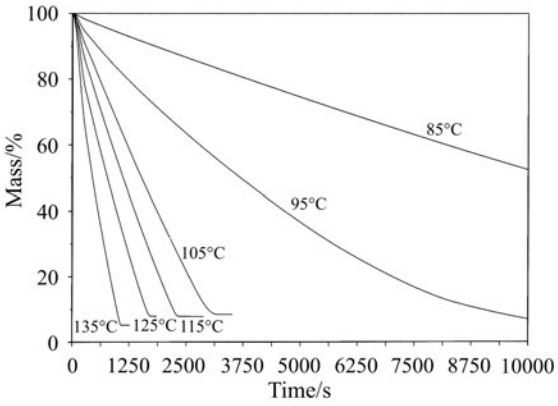

Fig. 4 Isothermal TG curves of TNAZ for several temperatures (sample mass 2.5 mg, open sample pan, nitrogen atmosphere)

From the TG curves given in Fig. 4, the degrees of conversion as a function of time were calculated using the following equation:

$$\alpha = \frac{m_i - m(t)}{m_i - m_f} \tag{1}$$

where m_i and m_f are sample initial and final masses respectively, and $m(t)$ is sample mass at a time t. The calculated $\alpha=f(t)$ curves are given in Fig. 5.

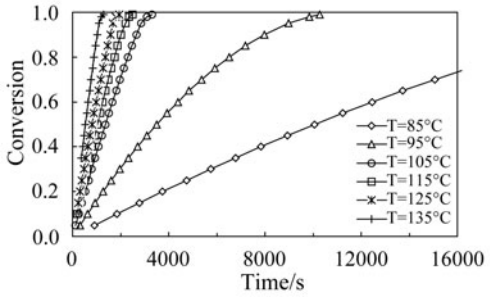

Fig. 5 TNAZ conversion *vs*. time for several temperatures

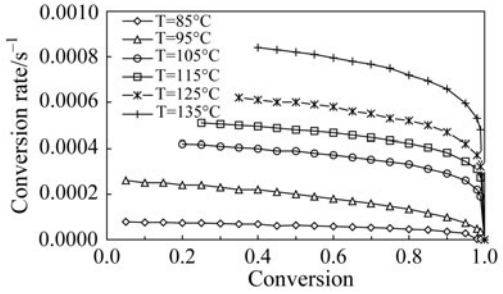

Fig. 6 Rate of conversion *vs*. conversion at different temperatures

The rates of conversion as a function of conversion, $d\alpha/dt=f(\alpha)$, were calculated from $\alpha=f(t)$ data given in Fig. 5, by the numerical derivation. The calculated $d\alpha/dt=f(\alpha)$ data are shown in Fig. 6.

It should be noted that the experimental procedure applied for the isothermal TG measurements causes some difficulties in data treatment, especially at higher temperatures. After the programmed temperature has been stabilised, the furnace has to be opened in order to insert the sample, which causes a considerable temperature drop. After the insertion of the sample and closing of the furnace, the temperature increases again and stabilises fully after 6–7 min (Fig. 7). During this temperature unstable period the TNAZ

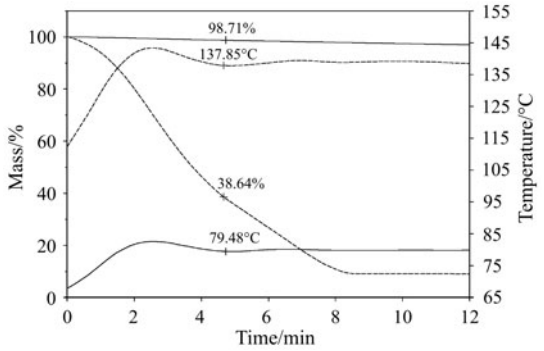

Fig. 7 Temperature stabilisation and sample mass *vs*. time after sample insertion in apparatus furnace preheated to 80 and 140°C isothermal temperatures

sample may sublimate and evaporate considerably. The sample mass loss during this period may range from only few percents (at low temperatures) to more than 50% at high temperatures (e.g. at 140°C, Fig. 7). That was the reason why this temperature unstable period was omitted from the calculation of the conversion rates (Fig. 6).

The shapes of the curves given in Figs 5 and 6, as well as the nature of the processes studied, suggest that the geometric kinetic models (Eqs (2) and (3)), commonly used to describe the phase-boundary controlled processes in which surface nucleation takes place extremely rapidly and the total process is governed by movement of the resulting interface towards the centre [22], can be used to described $d\alpha/dt=f(\alpha)$ dependency. Differential form of the general geometric kinetic model is:

$$\frac{d\alpha}{dt} = k(T)n(1-\alpha)^{(n-1)/n} \tag{2}$$

where $k(T)$ – temperature dependent rate constant, n – constant which for one-dimensional movement of reacting interface equals 1; for two-dimensional movement equals 2, and for three-dimensional movement equals 3,
while its integral form is:

$$k(T)t=1-(1-\alpha)^{1/n} \tag{3}$$

From Fig. 5 one may note that at temperatures above 100°C the dependence of conversion on time is almost linear within a broad range of conversions. This indicates that $\alpha=f(t)$ dependency may be described by a geometric model in which the reaction interface moves towards the centre according to one-dimensional movement model:

$$\alpha=k(T)t, \text{ or in differential form: } \frac{d\alpha}{dt}=k(T) \tag{4}$$

The above equation is known to be applicable for some cases of evaporation [22]. According to this model the conversion rate should be unchangeable with the conversion $[d\alpha/dt=k(T)]$. However, Fig. 7 shows that the conversion rate changes slightly with the conversion, indicating that this model may be applied to describe the evaporation process only within a limited range of conversion, i.e. with the limited accuracy.

In accordance with the above mentioned, the data given in Figs 5 and 6 were fitted to the general geometric kinetic model (Eqs (2) and (3)). The values of the rate constants and the constant n for different temperatures, obtained by the fitting procedure to both the differential and integral form of the kinetic equation applied, are given in Table 2.

According to the Arrhenius equation (Eq. (5)), the logarithmic values of the rate constants plotted *vs.* reciprocal temperature should give straight line, slope of which gives the activation energy:

$$\ln[k(T)]=\ln A-(E/RT) \tag{5}$$

The plot of the logarithmic values of the rate constant given *vs.* reciprocal temperatures is given in Fig. 8. It is clear from the figure that two regions with different slopes of $\ln[k(T)]=f(1/T)$ curve exist, which means that two regions with different activation energies exist. The point that separates these two regions corresponds to TNAZ melting temperature.

Table 2 Calculated values of $k(T)$ and n

Temperature/°C	Integral method			Differential method		
	Valid for	$k(T)/s^{-1}$	n	Valid for	$k(T)/s^{-1}$	n
			Sublimation			
75	$0.02<\alpha<0.06$	$1.46\cdot10^{-5}$	1.69	$0.05<\alpha<0.55$	$1.48\cdot10^{-5}$	1.59
80	$0.05<\alpha<0.85$	$2.19\cdot10^{-5}$	1.85	$0.05<\alpha<0.85$	$2.17\cdot10^{-5}$	1.79
85	$0.05<\alpha<0.99$	$3.65\cdot10^{-5}$	1.49	$0.05<\alpha<0.99$	$3.51\cdot10^{-5}$	1.49
90	$0.05<\alpha<0.99$	$5.43\cdot10^{-5}$	2.06	$0.20<\alpha<0.99$	$5.20\cdot10^{-4}$	1.97
95	$0.05<\alpha<0.99$	$8.78\cdot10^{-5}$	1.95	$0.20<\alpha<0.99$	$8.37\cdot10^{-4}$	1.82
	Mean value of n is: 1.81			Mean value of n is: 1.73		
			Evaporation			
100	$0.05<\alpha<0.99$	$2.40\cdot10^{-4}$	1.09	$0.20<\alpha<0.99$	$2.22\cdot10^{-4}$	1.08
105	$0.05<\alpha<0.99$	$3.25\cdot10^{-4}$	1.19	$0.20<\alpha<0.99$	$2.96\cdot10^{-4}$	1.19
110	$0.05<\alpha<0.99$	$2.70\cdot10^{-4}$	1.21	$0.50<\alpha<0.99$	$2.11\cdot10^{-4}$	1.36
115	$0.10<\alpha<0.99$	$4.22\cdot10^{-4}$	1.18	$0.30<\alpha<0.99$	$3.86\cdot10^{-4}$	1.18
120	$0.10<\alpha<0.99$	$7.08\cdot10^{-4}$	1.22	$0.35<\alpha<0.99$	$6.38\cdot10^{-4}$	1.23
125	$0.20<\alpha<0.99$	$6.33\cdot10^{-4}$	1.32	$0.40<\alpha<0.99$	$5.23\cdot10^{-4}$	1.35
130	$0.25<\alpha<0.99$	$1.07\cdot10^{-3}$	1.72	$0.50<\alpha<0.99$	$9.94\cdot10^{-4}$	1.65
135	$0.35<\alpha<0.99$	$8.41\cdot10^{-4}$	1.22	$0.55<\alpha<0.99$	$7.78\cdot10^{-4}$	1.16
140	$0.40<\alpha<0.99$	$1.88\cdot10^{-3}$	1.45	$0.70<\alpha<0.99$	$1.46\cdot10^{-3}$	1.41
	Mean value of n is: 1.29			Mean value of n is: 1.29		

The activation energies and pre-exponential factors for these two regions, calculated in accordance with the Arrhenius equation, are given in Table 3.

Table 3 Kinetic results for TNAZ sublimation and evaporation

Kinetic model	$75<T<95$°C (sublimation)	$100<T<140$°C (evaporation)
General geometric model (Eqs (2) and (3))	E^*=94 kJ mol^{-1} A^*=2.21· 10^9 s^{-1} n^*=1.77±0.21	E^*=60 kJ mol^{-1} A^*=4.80· 10^4 s^{-1} n^*=1.29±0.18
Two-dimensional movement, i.e. contracting cylinder (n=2, Eqs (6) and (7))	E^*=102 kJ mol^{-1} A^*=2.38· 10^{10} s^{-1} ($0.05<\alpha<0.99$)	
One-dimensional movement (n=1, Eq. (4))		E=66 kJ mol^{-1} A=3.69· 10^5 s^{-1} ($0.05–0.50<\alpha<0.90$)

*the mean value obtained from differential and integral equations

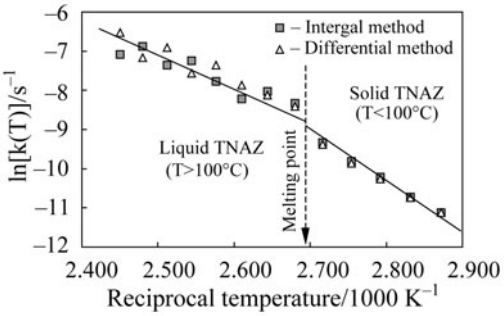

Fig. 8 Dependence of rate constant logarithm on reciprocal temperature

It can be noted from Tables 2 and 3 that the value of constant *n* changes also at the melting point (Fig. 9). The mean value of constant *n* at the sublimation region equals 1.77, while at the evaporation region constant *n* equals 1.29. Different values of constant *n* mean that different types of movement of the resulting interface towards the centre take place at the sublimation and evaporation processes.

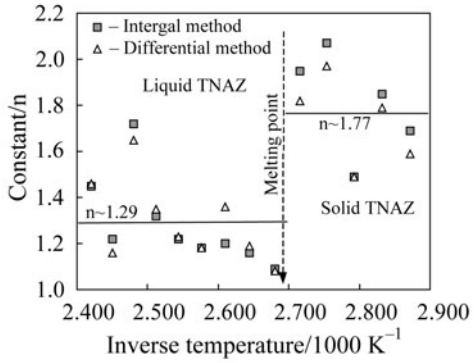

Fig. 9 Value of constant *n* for sublimation and evaporation processes

The fact that for the sublimation process constant *n* has a value close to 2 means that the reacting interface moves (approximately) according to the two-dimensional movement model (for which *n*=2), known also as the contracting cylinder reaction model:

$$\frac{d\alpha}{dt} = k(T)2(1-\alpha)^{1/2} \tag{6}$$

i.e. in the integral form:

$$k(T)t = 1-(1-\alpha)^{1/2} \tag{7}$$

The calculation of the kinetic parameters of the sublimation process according to the two-dimensional movement model (Eqs (6) and (7)) gives the activation energy of 102 kJ mol^{-1} and pre-exponential factor of $2.38 \cdot 10^{10}$ s^{-1} (Table 2), close to the values obtained by the general geometric model (Eqs (2) and (3)).

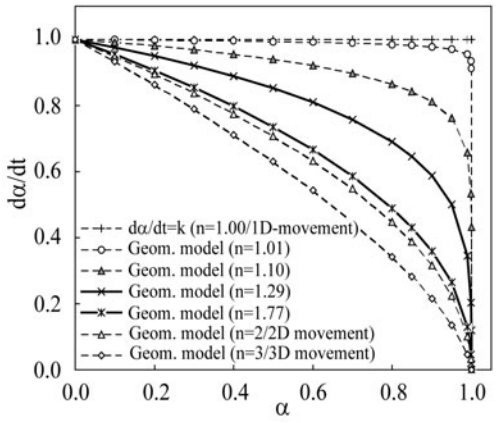

Fig. 10 Influence of constant *n* in the general geometric model (Eqs (2) and (3)) on the shape of $d\alpha/dt=f(\alpha)$ curves

Constant *n* for the evaporation process equals 1.29. It can be seen from Fig. 10 that $d\alpha/dt=f(\alpha)$ curve for the geometric model having $n=1.29$ lies between the two-dimensional and one-dimensional movement models, which may suggest that both of these reaction models take place simultaneously to a certain extent. It was found out by the curve fitting procedure that for the conversions lying between 0.05–0.5 and 0.9, $\alpha=f(t)$ dependency for the evaporation process may be satisfactory described by the one-dimensional movement reaction model (Eq. (4)). The activation energy of 66 kJ mol^{-1} was derived in this way (Table 2).

One may note that the values of constant *n* are considerably scattered (up to 15% with respect to the mean value), indicating that the influence of experimental parameters is considerable. It is not surprising if we know that the rate of conversion is influenced by a number of factors, such as reacting volume of the sample, specific surface of the sample, geometric factors, etc. [22, 23].

Enthalpy of evaporation and sublimation

The mass loss data obtained by the isothermal gravimetry were also treated in order to evaluate the enthalpy of evaporation ($\Delta_v H$). The enthalpy of evaporation was evaluated starting from the Langmuir equation [23, 24]:

$$-\frac{dm}{dt}=p\alpha_k\sqrt{\frac{M}{2\pi RT}} \tag{8}$$

where dm/dt – rate of mass loss per unit area, p – vapour pressure, M – molecular mass of the effusing vapour, R – gas constant, T – absolute temperature, α_k – vaporisation coefficient.

The above equation can be rearranged to give:

$$p=\frac{\sqrt{2\pi R}}{\alpha_k}\left(-\frac{dm}{dt}\sqrt{\left(\frac{T}{M}\right)}\right) \tag{9}$$

Equation (9) can be used for the calculation of the vapour pressure of an unknown material from TG isothermal measurements, if term $(\sqrt{2\pi R}/\alpha_k)$ is previously known, i.e. calibrated by a material with known vapour pressure.

The temperature dependence of the vapour pressure is given by the Clausius–Clapeyron equation, which can be written in the following form [23, 24]:

$$\ln(p)=B-\frac{\Delta H}{RT} \tag{10}$$

where ΔH is the molar enthalpy of evaporation ($\Delta_v H$), or molar enthalpy of sublimation ($\Delta_s H$) in the case of sublimation.

Combining Eqs (9) and (10) one obtains:

$$\ln\left(-\frac{dm}{dt}\sqrt{\frac{T}{M}}\right)=B-\frac{\Delta H}{RT}-\ln\left(\frac{\sqrt{2\pi R}}{\alpha_k}\right) \tag{11}$$

Since M, B and α_k have constant values, and taking that $(-dm/dt=k_m(d\alpha/dt))$, the above equation can be transformed in the following form:

$$\ln\left(\frac{d\alpha}{dt}\sqrt{T}\right)=B'-\frac{\Delta H}{RT} \tag{12}$$

where B' is a constant which includes all parameters that have constant values:

$$B'=B+\ln\left(\frac{\sqrt{2\pi R}}{\alpha_k}\right)+\ln(\sqrt{M})+\ln(k_m) \tag{13}$$

It follows from Eq. (12) that the plot of $[\ln(d\alpha/dt)/\sqrt{M}]$ *vs.* $1/T$ should give a straight line, the slope of which is $\Delta H/R$. It should be noted that Eq. (12) is analogous to the equation for the calculation of the enthalpy of sublimation and evaporation on the basis of TG temperature-jump measurements described by Flynn and Dickens [25], and Price [23, 24].

As mentioned earlier, $\alpha=f(t)$ dependency for the evaporation region, can be described satisfactorily by the one-dimensional movement reaction model (Eq. (4)), according to which the reaction rate does not depend on conversion: $(d\alpha/dt)=k(T)$. This is one of preconditions for the applicability of Eq. (12) for the calculation of the heat of evaporation.

In order to calculate the enthalpy of evaporation, $[\ln(d\alpha/dt)/\sqrt{T}]$ was plotted *vs.* $1/T$, and the enthalpy of vaporisation was calculated from the curve slope. In this way the enthalpy of vaporisation was found to be 66.8 kJ mol^{-1}.

From the first law of thermodynamics, and the fact that the enthalpies of sublimation ($\Delta_s H$) and evaporation ($\Delta_v H$) are the state functions, one can write for the melting temperature (T_m):

$$\Delta_s H(T_m)=\Delta_m H(T_m)+\Delta_v H(T_m) \quad (14)$$

According to Eq. (14), the enthalpy of sublimation at the melting temperature may be calculated from the enthalpy of melting and evaporation.

The enthalpy of melting and melting temperature were determined directly from the DSC endotherm peak (Fig. 1). As we found out in our previous paper, the melting temperature of TNAZ equals 100.59±0.21°C, while the melting enthalpy equals 153.3±1.6 J g^{-1} (i.e. 29.45±0.31 kJ mol^{-1}) [3].

The calculated enthalpy of evaporation of 66.8 kJ mol^{-1} was determined for the temperatures lying between 100 and 140°C. The enthalpy of evaporation at the melting temperature was calculated by the equations proposed by Chickos *et al*. [cited in 23]:

$$\Delta_v H(T_m)=\Delta_v H(T)-0.0540(T-T_m) \quad (15)$$

Taking that T=120°C, we have obtained that $\Delta_v H$(100.59°C) equals 65.8 kJ mol^{-1}. Substituting this value of the enthalpy of evaporation, and the enthalpy of melting into Eq. (14), the enthalpy of sublimation at the melting temperature was calculated to be: $\Delta_s H$(100.59°C)=95.3 kJ mol^{-1}. This value is close to the value of 106.2 kJ mol^{-1} calculated by Zeman and Krupka [26] from lattice energy.

Conclusions

The sublimation and evaporation of TNAZ were studied applying the isothermal and non-isothermal thermogravimetry measurements. The data presented in the paper show that TG measurements make possible not only derivation of the kinetic data but also derivation of the heats of evaporation and sublimation.

The activation energy values ranging between 94 and 102 kJ mol^{-1} were obtained for sublimation process, while for evaporation process the activation energy values were calculated to be between 60 and 81 kJ mol^{-1}.

The enthalpy of evaporation derived from the isothermal mass loss data equals 65.8 kJ mol^{-1}, while the enthalpy of sublimation of 95.3 kJ mol^{-1} was calculated from the enthalpies of melting and evaporation.

References

1 T. G. Archibald, R. Gilardi, K. Baum and C. George, J. Org. Chem., 55 (1990) 2920.
2 Z. Jalový, S. Zeman, P. Vávra, M. Sućeska, K. Dudek and M. Rajić, J. Energ. Mater., 19 (2001) 219.
3 M. Sućeska, M. Rajić, S. Zeman and Z. Jalový, J. Energ. Mater., 19 (2001) 241.
4 M. Sućeska, S. Zeman, M. Rajić and Z. Jalový, in Proc. 4th Int. Seminar 'New Trends in Research of Energetic Materials', Univ. of Pardubice, Czech Republic, April 11–12, 2001, p. 308.
5 R. I. Simpson, R. G. Garza, M. F. Foltz, D. I. Ornellas and P. A. Utriew, 'Characterisation of Tnaz', Rep. UCRL-ID-119572, Lawrence Livermore Lab., 1994.
6 R. L. McKenney, T. G. Floyd, W. E. Stevens, T. G. Archibald, A. P. Marchand, G. V. M. Sharma and S. G. Bott, J. Energ. Mater., 16 (1998) 1.

7 J. Zhang, R. Hu, Ch. Zhu, G. Feng and Q. Long, Thermochim. Acta, 298 (1997) 31.
8 G. A. Olah and D. R. Squire, 'Chemistry of Energetic Materials', Acad. Press, Inc., San Diego 1991, p. 27.
9 A. Sanderson, in Proc. 27th Int. Annual Conf. ICT, Karlsruhe, June 1996, p. 18/1.
10 J. C. Oxley, A. B. Kooh, R. Szekeres and W. Zheng, J. Phys. Chem., 98 (1994) 7004.
11 J. C. Oxley, J. Smith, W. Zheng, E. Rogers and M. Coburn, J. Phys. Chem., A 101 (1997) 4375.
12 J. Zhang, Ch. Zhu, X. Gong and H. Xiao, Wuli Huaxue Xuebao, 13 (1997) 612; Chem. Abstr., 127 (1997) 190 395.
13 K. Anderson, J. Homsy, R. Behrens and S. Bulusu, CPIA Publ., 657 (1997) 37.
14 N. R. Garland and H. H. Nelson, J. Phys. Chem., B 102 (1998) 2663.
15 S. Konrad and K. Doris, in Proc. 31st Annual Conf. ICT, Karlsruhe 2000, p.10/1.
16 K. Dudek, P. Mareček and P. Vávra, in Proc. 31st Int. Annual Conf. ICT, Karlsruhe 2000, p. 110/1.
17 M. D. Cook, J. Energ. Mater., 5 (1987) 257.
18 K. Schmid and D. Kaschmieder, in Proc. 31st Int. Annual Conf. ICT, Karlsruhe June 2000, p. 10/1.
19 J. H. Flynn and L. A. Wall, Polym. Lett., 4 (1966) 323.
20 J. H. Flynn, J. Thermal Anal., 27 (1983) 95.
21 M. D. Coburn, M. A. Hiskey, J. C. Oxley, J. L. Smith, W. Zheng and E. Rogers, J. Energ. Mater., 16 (1998) 73.
22 J. Šesták, Thermochim. Acta, 3 (1971) 1.
23 D. M. Price, J. Therm. Anal. Cal., 64 (2001) 315.
24 D. M. Price, Thermochim. Acta, 367–368 (2001) 253.
25 J. H. Flynn and B. Dickens, Thermochim. Acta, 15 (1976) 1.
26 S. Zeman and M. Krupka, HanNeng CaiLiao, 10 (2002) 27.